

Rate-dependent behaviour of fracture propagation in salt rock

**Proceedings of the 10th Conference on the Mechanical Behavior of Salt (SaltMech X),
Utrecht, The Netherlands, 06-08 July 2022**

Escanellas, Andreu; Cámara, Eduardo; Liaudat, J.; Carol, Ignacio

DOI

[10.1201/9781003295808-17](https://doi.org/10.1201/9781003295808-17)

Publication date

2022

Document Version

Final published version

Published in

The Mechanical Behavior of Salt X

Citation (APA)

Escanellas, A., Cámara, E., Liaudat, J., & Carol, I. (2022). Rate-dependent behaviour of fracture propagation in salt rock: Proceedings of the 10th Conference on the Mechanical Behavior of Salt (SaltMech X), Utrecht, The Netherlands, 06-08 July 2022. In J. H. P. de Bresser, M. R. Drury, P. A. Fokker, M. Gazzani, S. J. T. Hangx, A. R. Niemeijer, & C. J. Spiers (Eds.), *The Mechanical Behavior of Salt X: Proceedings of the 10th Conference on the Mechanical Behavior of Salt (SaltMech X), Utrecht, The Netherlands, 06-08 July 2022* (pp. 180-189). CRC Press / Balkema - Taylor & Francis Group. <https://doi.org/10.1201/9781003295808-17>

Important note

To cite this publication, please use the final published version (if applicable).
Please check the document version above.

Copyright

Other than for strictly personal use, it is not permitted to download, forward or distribute the text or part of it, without the consent of the author(s) and/or copyright holder(s), unless the work is under an open content license such as Creative Commons.

Takedown policy

Please contact us and provide details if you believe this document breaches copyrights.
We will remove access to the work immediately and investigate your claim.



Rate-dependent behaviour of fracture propagation in salt rock

Andreu Escanellas^{1}, Eduardo Cámara¹, Joaquín Liaudat² and Ignacio Carol¹*

¹ETSECCPB, Universitat Politècnica de Catalunya, Barcelona

²Geo-Engineering section, TU Delft, The Netherlands

* *andreu.escanellas@upc.edu*

ABSTRACT: This paper describes an on-going experimental and numerical modelling research project on salt rock specimens. The experimental part of the study consists of a number of Mode I fracture tests with the WST (Wedge-Splitting Test) configuration, which are performed at different loading rates and complemented by a series of standard uniaxial creep tests. The preliminary WST results show a greater mechanical fracture work accompanied with lower force peaks, for the slower tests. As a first attempt to represent the experimental results, an in-house Finite Element model has been used, which combines an inviscid discrete fracture approach with a Maxwell chain model for the continuum material. The simulations show a decrease of the mechanical work needed for opening the fracture and higher peak force, as foreseen by the ongoing experimental results, but not with the same intensity, which seems to indicate that work dissipation may not be caused exclusively by the bulk viscosity.

1 Introduction

The long-term deformations and stability of underground salt/potash mines are mainly determined by the viscous behaviour of the saline rock mass. As tunnels are excavated, deviatoric stresses are induced around the tunnel cross section, leading to the development of creep strains in the salt rock. Traditionally, it has been assumed that the main consequence of the creep deformation is the loss of serviceability of the mine due to the time-dependent convergences that progressively reduce the excavated cross-section. However, the development of creep deformations is associated to a progressive redistribution of stresses, which has the potential of inducing cracking and fracture in the salt rock, especially if discontinuities are already present in the rock mass. Consequently, a tunnel cross-section that is perfectly stable after the excavation may approach failure collapse as time goes by due to the propagation of fractures.

Because creep-fracture interactions have been often neglected, mine engineers have traditionally addressed the creep behaviour and the mechanical strength of the salt rock separately. On one hand, the creep behaviour is typically considered through simple visco-elastic models which make it possible to estimate the convergence rate and the possible effect on the tunnel serviceability. On the other hand, mechanical strength issues may be treated in ways similar to other rock materials, via strength criteria defined in the stress space. However, significant tunnel collapses have indicated that this approach may not be on the safe side (Whyatt & Varley 2008).

To the best of the authors' knowledge, very little has been published on the fracture mechanics of salt rock and the interaction between creep and fracture. Along this line, this paper describes an on-going experimental and numerical modelling research project which is carried out at UPC (Barcelona) on salt rock specimens from the mines in the region of Bages in Central Catalonia, Spain.

The experimental part of the study consists of a number of Mode I fracture tests at different loading rates, complemented by a series of standard uniaxial creep tests. The fracture tests were performed with the Wedge Splitting Test (WST) setup (see, e.g. Brühwiler & Wittmann 1990), at four different opening rates with the purpose of assessing the time dependency of parameters such as the tensile strength and the fracture energy.



In the numerical part of the study, the WST were simulated in order to aid the test interpretation and planning as suggested elsewhere (Liaudat et al. 2015). For this purpose, an in-house Finite Element model is used which allows to simulate WST within the discrete fracture approach.

2 Experimental evidence

2.1 Samples

The salt rock samples come from the Cardona saline formation. This formation, belonging to the Catalan potassium basin, formed between the Superior Eocene and Oligocene, when the Pyrenees rose, closing the oceanic communication of the mass of water that occupied what nowadays is the Ebro Valley. This closure gave place to a potent sedimentary series, where the layer of Halite can reach a thickness of more than 100 m.

Samples were extracted from Halite layers crossed by the mines in this region. Grain size range from <1 up to 20 mm, with no visible joints or preferential orientations. For the creep tests, cylindrical bore hole samples of 50 mm in diameter and 100 mm length were used. For the WST, prismatic blocks of 150x150x150 mm³ were cut.

2.2 Standard creep Tests

2.2.1 Methods

The aim of these creep tests is to aid the interpretation of the WSTs presented in the following Section 2.3, by assessing the uniaxial creep behaviour of the material. For this purpose, cylindrical samples were tested under three different load levels: 2.5 MPa, 5 MPa and 10 MPa. Since the WST at the lowest loading rate required approximately 12 hours, a total duration of the creep tests of 7 days was deemed sufficient for this study.

The vertical constant load was applied using an oedometer bench setting. Vertical displacements were recorded via LVDT transducers (± 2.5 mm, lineal error $< \pm 0.1\%$) aligned with the oedometer loading axis.

2.2.2 Results

Figure 1 shows the creep curves obtained in two different representations. The top plot shows the complete deformation curves, i.e. including the initial elastic deformation, in natural time scale. The bottom plot shows the steady state creep deformation, i.e. after deducting the initial elastic deformation, in logarithmic time scale.

Observing the bottom plot at the end of the tests, it is apparent that the time-dependent strain obtained for 5 MPa is approximately twice the strain obtained for 2.5 MPa. Therefore, creep for compressive loading under 5 MPa may preliminary be considered as proportional to the applied load level, i.e. the linear creep assumption may be valid. In contrast, the creep obtained for 10 MPa is about 6 times the creep observed for 5 MPa, and consequently, for the purpose of the current study, creep under uniaxial stress of 5 MPa may be considered preliminarily as linear creep. This limit value of 5 MPa for the linear range of creep seems to be in agreement with other experimental observations in similar time ranges, e.g. Wang et al. (2022).

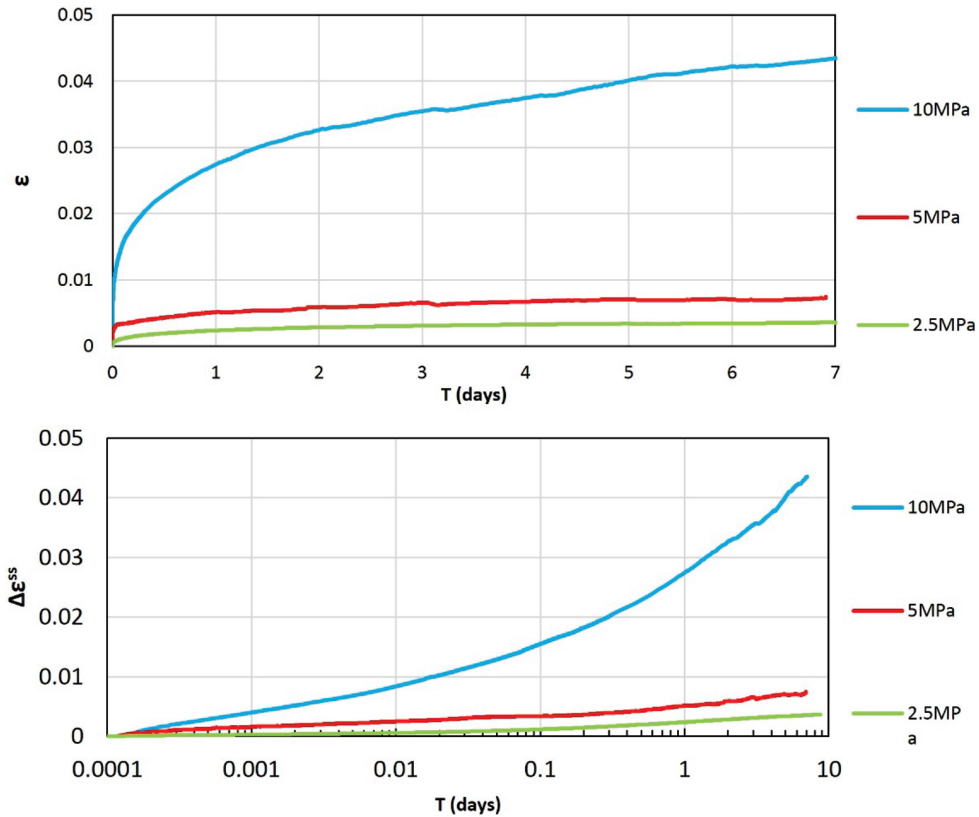


Figure 1: Uniaxial creep curves for three different load levels. Top, complete deformation (ϵ) curves in natural time scale. Bottom, steady state creep ($\Delta\epsilon^{ss}$) curves in logarithmic time scale.

2.3 Wedge Splitting Tests (WST)

2.3.1 Methods

The WST is a method to generate stable fracture propagation in quasi-brittle materials, e.g. rock or concrete, to determine fracture mechanics parameters in mode I such as the fracture toughness or the specific fracture energy (e.g. see Brühwiler & Wittmann 1990). The specifics of the setup used for this study are schematically depicted in Figure 2 (left). A rectangular notch and a groove are cut in the cubic specimens in order to apply the splitting force and to localise the fracture. A pair of steel L-profiles equipped with roller bearings is affixed to both sides of the notch. Lateral opening displacement of the rollers is imposed through a wedge moving vertically down. From the $F_H - COD$ (Horizontal splitting force – Crack Opening Displacement) response of the specimen, the specific fracture energy is determined. Moreover, with this setting, the tensile strength can also be derived via numerical back analysis.

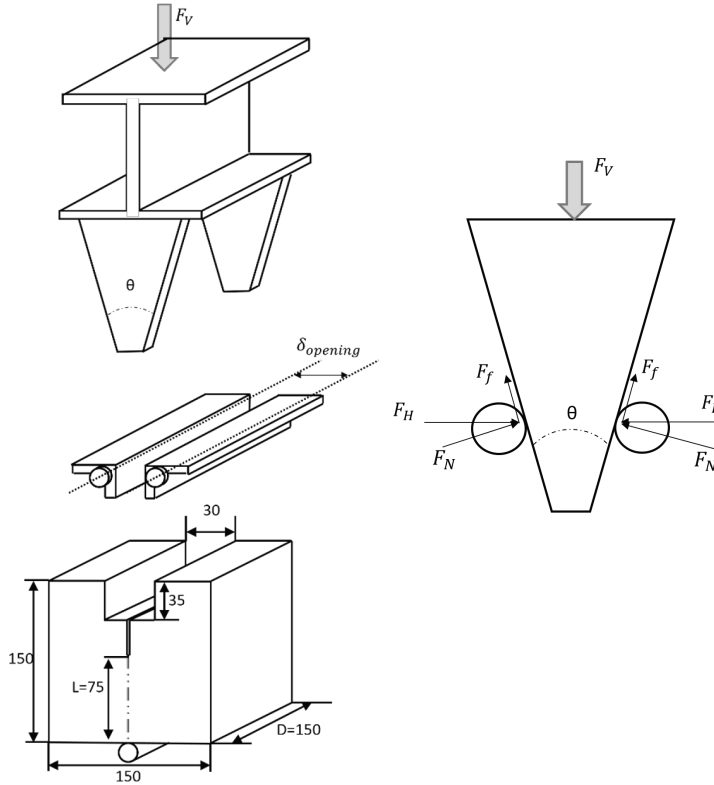


Figure 2: Wedge Splitting Test setup (left) and graphical force decomposition at the wedge-roller bearing contacts (right).

Figure 2 (right) shows a free body diagram of forces on the wedge. The horizontal force applied to the specimen is calculated by means of Equation (1), where F_V is the vertical load applied, θ is the wedge angle and μ is the coefficient of friction between wedge and roller.

$$F_H = \frac{1 - \mu \tan \varphi}{2(\mu + \tan \varphi)} F_V \quad (1)$$

If the fracture process is stable, the mechanical work required to create a unit area of fracture (\tilde{G}_f^I [J/m²]) can be obtained from the $F_H - COD$ response of the specimen using Equation (2), where A_f is the surface of the ligament area ($A_f = L \cdot D$, as in Figure 2).

$$\tilde{G}_f^I = \frac{1}{A_f} \int_0^\infty F_H dCOD \quad (2)$$

For a material with negligible creep deformation, \tilde{G}_f^I can be identified with the specific fracture energy of the material G_f^I , a rate-independent material parameter. In the case of salt rock, in contrast, part of the invested mechanical work will be spent in creep deformations and, consequently, \tilde{G}_f^I is expected to be a rate dependent value.

The testing system used consisted of a loading frame, a load cell, two displacement measurement devices and data acquisition equipment:

- Loading frame – ELE Digital Tritest 100 (loading capacity 500kN). Load cell – UtilCell 610 (nominal load 25 kN, linearity error $< \pm 0.25\%$ F.S.) with signal conditioning amplifiers Krenel CEL/M010.

- Displacement measuring devices – Two LVDT displacement transducers RDP GT2500, $\pm 2.5\text{mm}$ (linearity error $< \pm 0.1\%$ F.S.), with signal conditioning amplifiers RDP S7AC, were used in the axis of the horizontal splitting force, one on each side of the specimen (COD1 on side 1, COD2 on side 2).

- Data acquisition – ELE automatic data acquisition unit.

2.3.2 Results

In order to investigate the effect of the loading rate on the $F_H - COD$ response curve, four WSTs were performed with different COD rates, namely: 5, 0.625, 0.078 and 0.011 mm/min. The obtained curves are given in Figure 3. It can be readily appreciated in this plot that as the COD rate decreases, the peak value of the F_H decreases but the area under the curves (the spent mechanical work) increases.

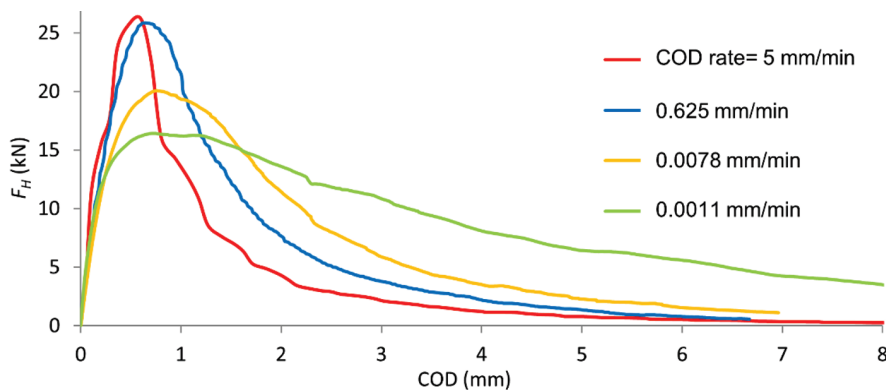


Figure 3: Wedge Splitting Test curves for different COD rates.

3 Discussion

As a first (simplest) interpretation, the observed effect of the COD rate on the WST curves could be attributed solely to the development of creep deformations in the bulk material. In order to test this hypothesis, the performed WSTs are simulated with a Finite Element numerical model, as has been done before for other types of rock by some of the authors (Liaudat et al. 2015; Liaudat et al. 2017).

3.1 The numerical model

The model consists of continuum elements for the bulk of the salt rock, while the fracture is represented via zero-thickness interface elements pre-inserted along the fracture path, which are equipped with a mechanical constitutive law based in the non-linear fracture mechanics theory (Carol et al. 1997). This constitutive law has an analogous structure to traditional elasto-plasticity theory using a yielding surface in the stress plane as a criterion for fracturing. The parameters that describe the yielding surface (F) depend on the fracture work (W^{ct}) as history variable. Thus, when fracture work reaches the value of the fracture energy of the material (G_f^I), tensile strength has totally vanished. The main aspects of this law are summarised in Figure 4.

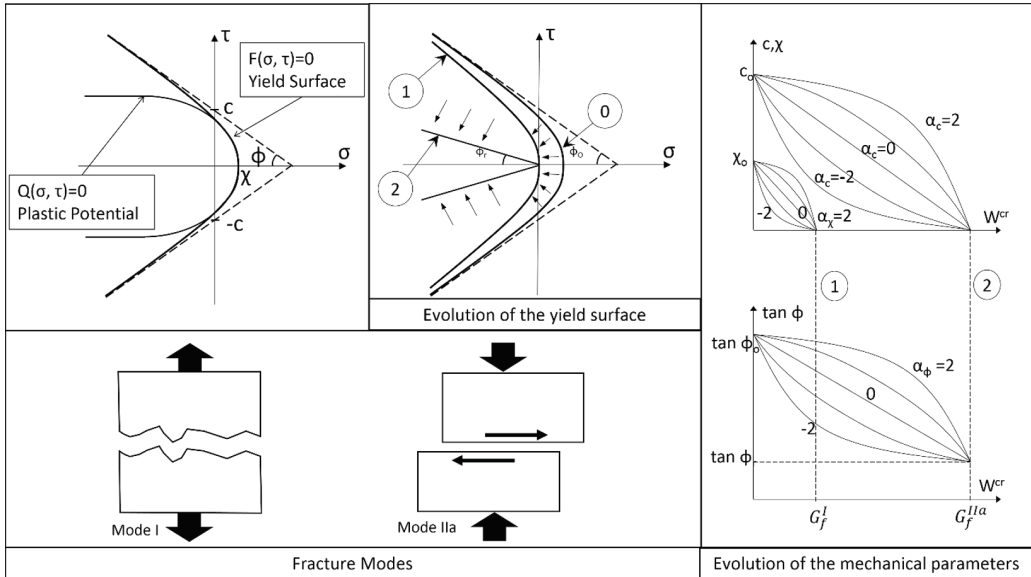


Figure 4. Fracture-based elasto-plastic constitutive law for interface element. After Carol et al. (1997). Being c , shear strength, χ , tensile strength, ϕ , internal friction angle, G_f^I , fracture energy in mode I, G_f^{IIa} fracture energy for mode IIa, α_c , α_χ and α_ϕ , shape parameters for the evolution of mechanical parameters.

The FE mesh and boundary conditions used for the calculations are depicted in Figure 4. The geometry corresponds to the cross section of a generic specimens of 150x150 mm. The dark blue elements represent the loading plates, and the magenta elements are used to represent the compliance of the loading system. The red arrows represent the imposed horizontal displacements.

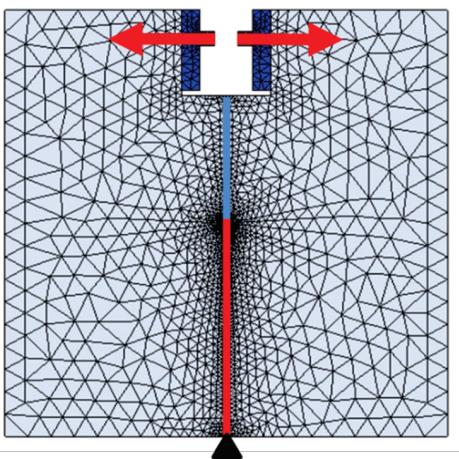


Figure 5: Finite Element mesh and boundary conditions of the problem.

In order to calibrate the parameters of the fracture constitutive law, a first simulation is performed of the WST test with highest loading rate, by using linear elasticity for the continuum elements representing the salt rock. This corresponds to assuming that in this fast loading

case viscous deformations are very small and may be neglected, which may be only approximate but is a simple first approach to determine fracture parameters. Figure 5 shows the experimental WST curve for the highest COD rate together with the fitted numerical curve, using elastic parameters $E = 900 \text{ MPa}$, $\nu = 0.3$. The calibrated parameters are the tensile strength $\chi_0 = 3.15 \text{ MPa}$ and the specific fracture energy $G_f^I = 400 \text{ J/m}^2$. The rest of the constitutive parameters are not relevant since shear stresses cannot be developed due to the symmetry of the problem.

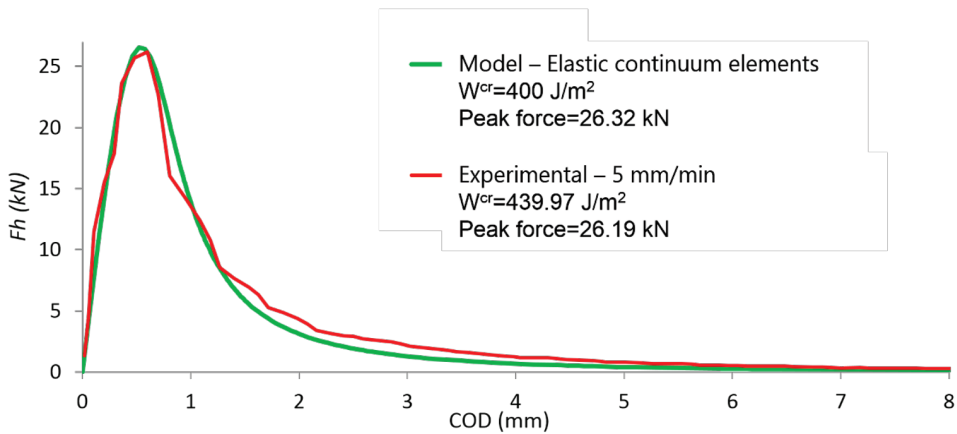


Figure 6: Wedge Splitting Test curves: experimental for 5 mm/min COD rate and numerical modelling using a linear elastic law for representing the salt rock.

Once these parameters have been calibrated, a second set of simulations have been performed using a Maxwell chain visco-elastic constitutive law for the continuum elements representing the salt rock, in order to reproduce the creep behaviour reported in Section 2.2. This combination of visco-elastic continuum elements and rate-independent interface element has been previously proposed by López et al. (2001) for modelling combined creep and cracking in concrete. The visco-elastic law parameters were obtained by fitting the data from the uniaxial creep tests under 2.5 MPa (Section 2.2) using the method proposed by Bažant (1982).

Figure 6 shows the WST curves obtained with the model for the four experimental COD rates. For comparison, the experimental WST curves are plotted (in grey dashed lines) together with the numerical curves. Both the numerical and experimental WST results are summarised in Figure 7 in terms of the peak splitting force (F_H) and the apparent fracture energy (\tilde{G}_f^I) as functions of the COD rate.

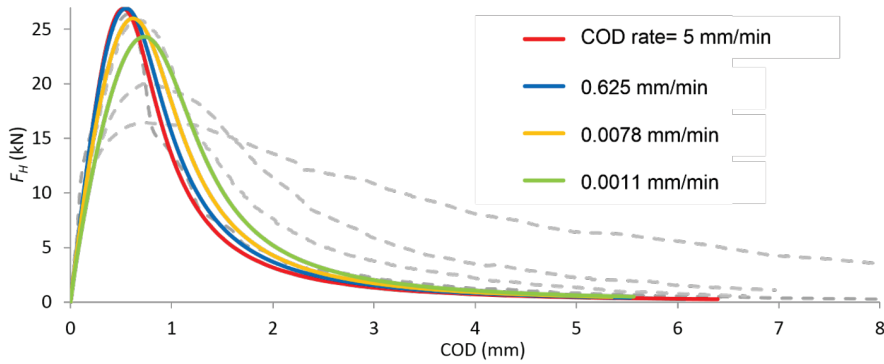


Figure 7: Numerical Wedge Splitting Test curves for different COD rates using a visco-elastic constitutive law for representing the salt rock. The dashed lines correspond to the experimental curves in Figure 3.

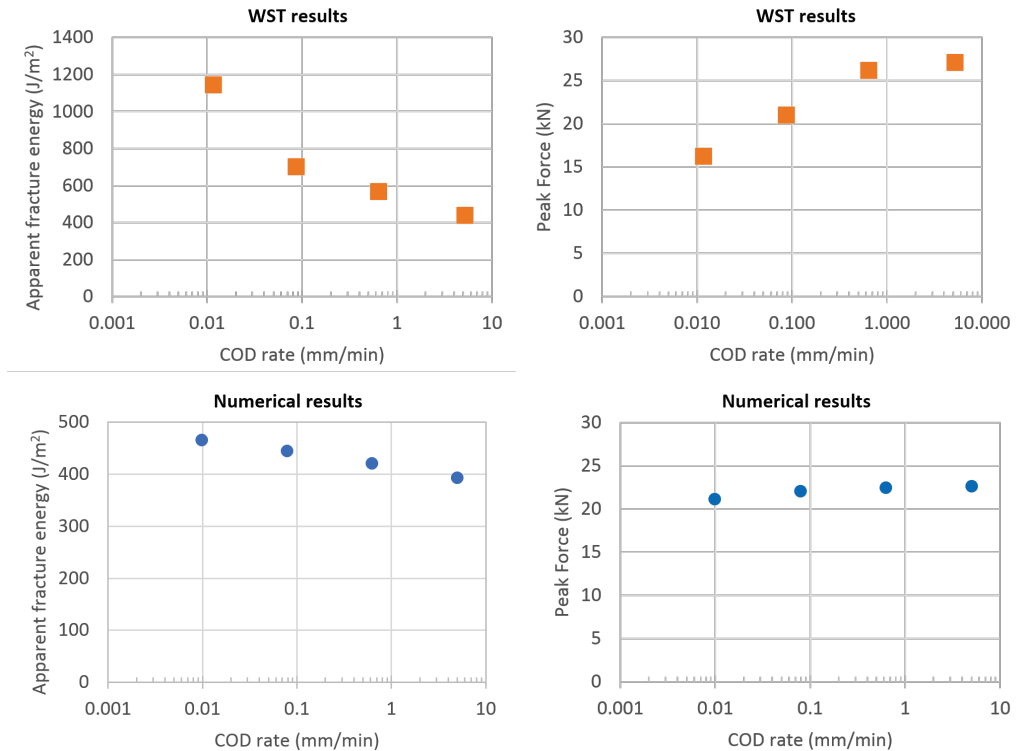


Figure 8: Peak horizontal force (F_H) and apparent fracture energy (\tilde{G}_f^I) as a function of the COD rate. Top, experimental results. Bottom, numerical modelling results.

In Fig. 6 and 7, it can be observed that the numerical model was able to qualitatively reproduce the main trends observed in the experiments, i.e. the reduction of the peak splitting force and the increase of the apparent fracture energy for decreasing loading rates. However, the model failed to quantitatively capture the experimental response. This analysis seems to indicate that the effect of the loading rate on the WST cannot be attributed solely to the creep deformations of the saline rock on both sides of the fracture path, and that the loading rate could have an effect on the development of the fracture itself. In the proposed numerical modelling approach,



introducing that effect would require a new rate-dependent constitutive law for the interface elements which would combine fracture/damage and viscous behaviour.

4 Concluding remarks

- The effect of the loading rate on the development of Mode I fractures in salt rock is being investigated by means of WST tests with different COD rates.
- Preliminary results indicate that the peak splitting force decreases, and apparent fracture energy increases as the COD decreases. Further testing is needed to confirm these trends and assess the variability of the results.
- Numerical modelling analysis of the experimental results seems to indicate that these effects cannot be only attributed to the development of creep deformations in bulk salt rock, and that the viscous effects would need to be introduced in the discrete fracture law as well.

Acknowledgements

This work was partially supported by research grants BIA2016-76543-R and PID-2020-117933RB-100 from MEC (Madrid), which include European FEDER funds, as well as grant SGR2017-1153 from Generalitat de Catalunya (Barcelona) The first author also acknowledges his FI scholarship (FI-AGAUR 2021) from Secretaria d'Universitats i Recerca de la Generalitat de Catalunya, which includes European Social Funds.

References

- BAŽANT, Z. 1982. Mathematical models for creep and shrinkage of concrete. Creep and Shrinkage in concrete structures, New York, NY: John Wiley & Sons, 1982, pp. 263-256.
- BRÜHWILER, E. & WITTMANN, F. 1990. The wedge splitting test, a new method of performing stable fracture mechanics tests. *Engineering Fracture Mechanics*, vol. 35, 117– 125.
- CAROL, I., PRAT, P. C. & LÓPEZ, C. M. 1997. Normal/Shear Cracking Model: Application to Discrete Crack Analysis. *Journal of Engineering Mechanics*, 123(8), 765–773.
- LIAUDAT, J., GAROLERA, D., MARTÍNEZ, A., CAROL, I., LAKSHMIKANTHA, M. R. & ALVARELLOS, J. 2015. Numerical modelling of the Wedge Splitting Test in rock specimens, using fracture-based zero-thickness interface elements. E. Oñate, D. R. J. Owen, D. Peric, & M. Chiumenti (Eds.), XIII International Conference on Computational Plasticity - Fundamentals and Applications (COMPLAS XIII), pp. 974–981. International Center for Numerical Methods in Engineering (CIMNE).
- LIAUDAT, J., GAROLERA, D., CAROL, I., LAKSHMIKANTHA, M. R. & ALVARELLOS, J. 2017. Avoiding fracture instability in Wedge Splitting Tests by means of numerical simulations. E. Oñate, D.R.J. Owen, D. Peric & M. Chiumenti (Eds.), XIV International Conference on Computational Plasticity. Fundamentals and Applications (COMPLAS XIV), pp. 514-521. International Center for Numerical Methods in Engineering (CIMNE), Barcelona.
- LÓPEZ, C. M., CAROL, I. & MURCIA, J. 2011. Mesostructural modeling of basic creep at various stress levels. *Creep, Shrinkage and Durability Mechanics of Concrete and other Quasi-Brittle materials*, 101-106.
- WANG J., ZHANG Q., SONG Z., FENG S. & ZHANG Y. 2021 Nonlinear creep model of salt rock used for displacement prediction of salt cavern gas storage, *Journal of Energy Storage* 48
- WHYATT, J. & VARLEY, F. 2008. Catastrophic Failures of Underground Evaporite Mines. *Proceedings of the 27th International Conference on Ground Control in Mining*; July 29 - July 31, 2008, Morgantown, West Virginia. Peng S.S., Mark C, Finfinger G.L., Tadolini



S.C., Khair A.W., Heasley K.A., Luo-Y, eds., Morgantown, WV: West Virginia University, 113–122.